

## CO<sub>2</sub> capture performance of cement-modified carbide slag

Xiaotong Ma\*, Yingjie Li\*,†, Changyun Chi\*, Wan Zhang\*, and Zeyan Wang\*\*

\*School of Energy and Power Engineering, Shandong University, Jinan 250061, China

\*\*State Key Laboratory of Crystal Materials, Shandong University, Jinan 250100, China

(Received 15 July 2016 • accepted 5 November 2016)

**Abstract**—A novel and low-cost synthetic CO<sub>2</sub> sorbent for calcium looping process, cement-modified carbide slag (CMCS), was synthesized from carbide slag, aluminate cement and by-product of biodiesel by combustion. The effects of synthesis conditions such as combustion temperature, combustion duration, hydration, by-product of biodiesel and cement addition and regeneration temperature on CO<sub>2</sub> capture performance of CMCS were investigated. The comprehensively optimum preparation conditions of CMCS were obtained. The highest CO<sub>2</sub> capture capacity is 0.62 g/g after 10 cycles, which is 2.18 times as high as that of carbide slag. The addition of aluminate cement improves the CO<sub>2</sub> capture performance of CMCS, while excessive aluminate cement is adverse for CO<sub>2</sub> capture due to the reduced CaO content in CMCS. The addition of by-product of biodiesel contributes to a uniform sol mixing of carbide slag and cement. The CMCS exhibits higher carbonation and calcination rates than CS. The porous and stable pore structure leads to the better CO<sub>2</sub> capture performance and cyclic stability of CMCS.

Keywords: Cement, Carbide Slag, By-product of Biodiesel, Calcium Looping, CO<sub>2</sub> Capture

### INTRODUCTION

Calcium looping is one of the most promising technologies for large-scale CO<sub>2</sub> capture due to its low operation cost and other advantages [1-4]. The calcium looping process is achieved when CaO-based sorbent absorbs CO<sub>2</sub> in a carbonator to form CaCO<sub>3</sub>, and the CaCO<sub>3</sub> is then transported to a calciner for regeneration of CaO and enrichment of CO<sub>2</sub>. However, the deactivation of CaO-based sorbent over the multiple carbonation/calcination cycles due to sintering and aggregation is the main barrier which limits the large-scale applications [5,6]. To improve the sintering and aggregation resistance of CaO-based sorbents, the additives such as Y<sub>2</sub>O<sub>3</sub>, ZrO<sub>2</sub> and SiO<sub>2</sub> which can stabilize the mechanic structure of sorbents and the various methods such as sol-gel, wet mixing and dry physical mix which can make CaO disperse into inert supports have been comprehensively studied [7-10].

Researches have shown that calcium aluminates as inert supports are effective to stabilize pore structure of CaO, which slows down sintering of CaO crystallites [11-13]. Different modification and synthesis methods lead to various types of calcium aluminates and difference in the structure of sorbents. Zhang et al. [11] synthesized CaO/Ca<sub>3</sub>Al<sub>2</sub>O<sub>6</sub> sorbents using citric acid, aluminum nitrate and CaCO<sub>3</sub> through the citrate preparation route. The CO<sub>2</sub> capture capacity of sorbent with 9% Al<sub>2</sub>O<sub>3</sub> additive was 0.41 g/g over 50 cycles, which was double that of untreated CaCO<sub>3</sub>. Li et al. [14]

found that Ca<sub>3</sub>Al<sub>2</sub>O<sub>6</sub> was formed in the synthesized sorbent prepared from carbide slag, aluminum nitrate hydrate and glycerol by combustion method, which was due to the reaction between CaO and Al<sub>2</sub>O<sub>3</sub>. Zhang et al. [15] spray-dried sol mixture of CaO and Al(NO<sub>3</sub>)<sub>3</sub>·9H<sub>2</sub>O and obtained Ca<sub>12</sub>Al<sub>14</sub>O<sub>33</sub> during high temperature calcination as the inert solid support, exhibiting the carbonation conversion twice as high as that of limestone after 13 cycles. Zhou et al. [16] concluded that CaO/Ca<sub>9</sub>Al<sub>6</sub>O<sub>18</sub> sorbent with CaO content of 80 wt% derived from calcium citrate and aluminum nitrate exhibited the best performance for CO<sub>2</sub> capture. They claimed that the inert support materials separating CaO particles were not all the same and could be Al<sub>2</sub>O<sub>3</sub>, Ca<sub>12</sub>Al<sub>14</sub>O<sub>33</sub> or Ca<sub>9</sub>Al<sub>6</sub>O<sub>18</sub>, depending on the diffusion resistance of Ca<sup>2+</sup> into Al<sub>2</sub>O<sub>3</sub> during the solid-state reaction when different calcium and aluminum precursors were used. Chen et al. [17] obtained another aluminum nitrate, Ca<sub>3</sub>Al<sub>10</sub>O<sub>18</sub>, when sorbent was modified with attapulgite by hydration, due to the decrease in temperature for the solid-state reaction during the process of hydration. Aluminate cement, as an important cementitious material, has been widely applied in civil construction, water conservation, national defense and other engineering projects. Billion tons of aluminate cement is produced every year. It is low-cost and desirable when resistance is required to prevent corrosion and chemicals as well as refractory properties, which are beneficial for stabilizing the pore structure under high temperature condition, and thus it is promising as supporting material for Ca-based sorbents [18-20]. They usually contain impurities and a wide range of Al<sub>2</sub>O<sub>3</sub>/CaO ratios, depending on purity of the aluminum source used and application. This favorable performance of CaO-based sorbents supported by calcium aluminate cements was explained by formation of mayenite (Ca<sub>12</sub>Al<sub>14</sub>O<sub>33</sub>) [21,22]. However, the collapse and blockage of the pore structure, resulting in the decay in CO<sub>2</sub> capture capacities of these proposed sorbents, is still a matter of concern for

†To whom correspondence should be addressed.

E-mail: liyj@sdu.edu.cn

\*This work was presented at the 11<sup>th</sup> China-Korea Workshop on Clean Energy Technology held at Southeast University, China, Sep. 20-23, 2016.

Copyright by The Korean Institute of Chemical Engineers.

their large-scale applications.

The mass use of limestone as CaO precursor is supposed to affect the geological environment in the process of mining. Our previous works have showed that carbide slag (CS, for short) as an industrial waste dumped from a chlor-alkali plant, could be used to capture CO<sub>2</sub> during the calcium looping cycles [23-26]. Thus, the utilization of CS can avoid the irreparable damage of consuming limestone mine to the environment. The main composition of CS is Ca(OH)<sub>2</sub>. CS is a cheap material that can be also used as a calcium precursor for the preparation of inert material supported CO<sub>2</sub> sorbent with high activity. The key for the obviously positive effect on CO<sub>2</sub> capture capacity is the uniform mix of CS and inert materials according to the results of our recent study [27]. It is not surprising that sol mixing when at least one of the precursors is soluble powder is easier to mix well than suspension mixing when all precursors are insoluble powder [28]. Ca(OH)<sub>2</sub> in CS is soluble in glycerol, which can be replaced by by-product of biodiesel (>90 wt% glycerol content) obtained from the transesterification process for biodiesel production [29]. Biodiesel has become one of the promising alternative fuels because it is renewable and environmentally friendly [30]. Its current output stands at about 2-3×10<sup>7</sup> tons per year. About 0.3 kg of glycerol accompanies each gallon of biodiesel during the transesterification process, which means that billion gallons of glycerol contained in the by-product of biodiesel are produced annually. Thus, the cost for synthesizing sorbents can be further reduced if by-product of biodiesel can be reused in the preparation process of the synthetic sorbent for CO<sub>2</sub> capture.

We used CS and commercial aluminate cement (cement, for short) as calcium precursor and supporting material, respectively, for their low cost to synthesize economical sorbents. The by-product of biodiesel was added to realize sol mixing between the soluble Ca(OH)<sub>2</sub> in CS and insoluble cement to form a sorbent comprising CaO surrounded by uniformly distributed cement. Our main objective was to fabricate a novel CO<sub>2</sub> sorbent with high CO<sub>2</sub> capture capacity and sintering-resistance by combustion method. The CO<sub>2</sub> capture behaviour of cement-modified CS (CMCS, for short) was investigated and compared with original CS during the repetitive carbonation/calcination cycles. The effects of preparation process of CMCS including combustion temperature, combustion duration, by-product of biodiesel addition, hydration and cement addition and calcination temperature on its CO<sub>2</sub> capture performance were discussed during the calcium looping process.

## EXPERIMENTAL

### 1. Sorbent Preparation

Raw CS was sampled from a chlor-alkali plant in Shandong Province, China and the samples that passed through the 0.125 mm sieve was collected. The chemical components of CS are shown in Table 1. The cement was sampled from a cement plant in Jinan,

**Table 1. Chemical components of CS (wt%)**

CaO	MgO	SiO <sub>2</sub>	Al <sub>2</sub> O <sub>3</sub>	Fe <sub>2</sub> O <sub>3</sub>	SrO	Ti <sub>2</sub> O	Others	Loss on ignition
69.52	0.02	2.34	1.52	0.17	0.03	0.03	0.57	25.80

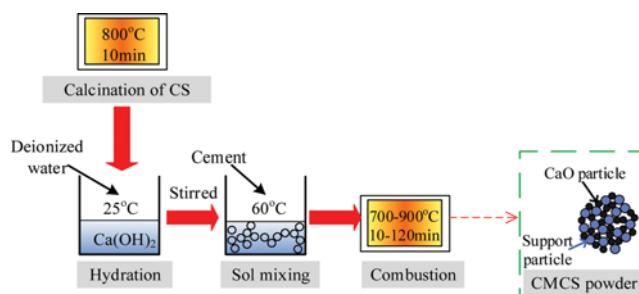


**Fig. 1. Four-step preparation process of CMCS.**

Shandong Province, China, containing Al<sub>2</sub>O<sub>3</sub> of 39 wt%. The by-product of biodiesel (>90 wt% glycerol content) was obtained from the transesterification process of peanut oil (CaO addition percentage of 6%, reaction temperature of 64 °C, molar ratio of methanol to peanut oil of 12 : 1 and reaction time of 2 h, CaO as catalyst) [29].

The preparation of the sorbents includes four steps: calcination, hydration, sol-mixing and combustion, as shown in Fig. 1. CS was calcined at 800 °C for 10 min. The obtained CaO material was treated in water. 600 mg calcined CS was put in a glass beaker after cooling and deionized water was added into the beaker dropwise to avoid the heat released due to the exothermal hydration process of CaO. Weighed amounts of cement at mass ratios of CaO to cement of 95 : 5, 85 : 15 and 75 : 25 and 60 ml by-product of biodiesel were added and stirred at 60 °C for 60 min for sol mixing. Then it was placed in a muffle furnace for combustion at 700-900 °C under air for 10-120 min. The obtained sorbent was the cement-modified carbide slag (CMCS). Then it was collected and subjected to cyclic carbonation/calcination performance test. The cement-modified carbide slag containing 5, 15, and 25 wt% cement was denoted as CMCS-5, CMCS-15 and CMCS-25, respectively. To study the effect of hydration of calcined CS on CO<sub>2</sub> capture of CMCS, CMCS without hydration step was obtained by following the same procedure mentioned above, except that raw CS was directly mixed with the same amounts of cement, deionized water and by-product of biodiesel. Also as a comparison, calcined CS after hydration was subjected to cycles. Similarly, CMCS without the addition of by-product of biodiesel and CS with the addition of by-product of biodiesel (i.e., CMCS without the addition of cement) was also prepared.

### 2. CO<sub>2</sub> Capture Test and Characterization

The CO<sub>2</sub> capture test was carried out in a dual fixed-bed reactor including a carbonator and a calciner operated under atmospheric pressure. The experiments were done with carbonation in 15% CO<sub>2</sub> (N<sub>2</sub> balance) at 700 °C and calcination in 99.999% N<sub>2</sub> at 850-950 °C. The reaction gas flow was 1 L, which was controlled by mass flowmeters. The CO<sub>2</sub> capture capacities were calculated on the basis of mass change as follows:

$$C_N = \frac{m_N - m_{cal, N}}{m_0} \quad (1)$$

where,  $N$  is the number of carbonation/calcination cycles.  $C_N$  represents the CO<sub>2</sub> capture capacity of the sorbent after  $N$  cycles, i.e., CO<sub>2</sub> adsorption amount per unit mass of the sorbent, g (CO<sub>2</sub>)/g (sorbent).  $m_0$  is the mass of the initial sorbent sample, g.  $m_N$  is the

mass of the sorbent after the  $N$ th carbonation,  $g$ .  $m_{cal,N}$  is the mass of the sorbent after the  $N$ th calcination,  $g$ .

The  $CO_2$  absorption tests of CMCS-5 and CS in the 1st and 11th cycles were performed in a Mettler Toledo TGA/SDTA851<sup>e</sup> thermal gravimetric analyzer (TGA). The samples which had experienced 0 and 10 carbonation/calcination cycles were sampled from fixed-bed reactor (carbonation: 15%  $CO_2$ , 700 °C, 20 min; calcination: 99.999%  $N_2$ , 850 °C, 10 min). And then about 5 mg of the cycled sample and the uncycled sample were placed into a ceramic pan and sent to TGA, respectively. The heating process of TGA was conducted in  $N_2$  at heating rate of 50 °C/min. A whole cycle was done in TGA under the same carbonation condition as that in the dual fixed-bed reactor to comprehensively study  $CO_2$  capture characteristics of the sorbents. The mixed gas of 15%  $CO_2/N_2$  was sent to the TGA (the total gas flow was kept at 120 mL/min) as soon as the temperature reached 700 °C. Then the reaction gas was switched to 99.999%  $N_2$  again 20 min later. The  $CO_2$  capture capacity of the sample in TGA was calculated according to Eq. (1). The decomposition ratio of the carbonated sample was calculated according to Eq. (2). The carbonation rate of the calcined sample and calcination rate of the carbonated sample were computed with Eqs. (3) and (4), respectively.

$$R_{N,t} = \frac{m_{N,t1} - m_{N,t}}{m_{N,t1} - m_{N,t2}} \quad (2)$$

$$\mu_{N,t} = \frac{d(m_{N,t} - m_{N,t-1})}{m_0 dt} \quad (0 < t < t_1) \quad (3)$$

$$\nu_{N,t} = \frac{d(m_{N,t} - m_{N,t-1})}{m_0 dt} \quad (t_1 \leq t \leq t_2) \quad (4)$$

where  $R_{N,t}$  represents decomposition ratio of the sorbent at  $t$  in the  $N$ th cycle (%).  $m_{N,t}$  is the mass of the sorbent at  $t$  during the  $N$ th cycle ( $g$ ).  $t_1$  and  $t_2$  are the end times of carbonation and calcination process, respectively (s).  $\mu_{N,t}$  and  $\nu_{N,t}$  represent carbonation and calcination rates at  $t$  in the  $N$ th cycle, respectively ( $s^{-1}$ ).

The sample morphologies were observed with an SUPRATM 55 field emission scanning electron microscope (SEM) before and after multiple carbonation/calcination cycles.

## RESULTS AND DISCUSSION

### 1. Effect of Cement Addition in Preparation Process of CMCS on $CO_2$ Capture

The cyclic  $CO_2$  capture capacities of CMCS containing various amounts of cement (5, 15, 25 wt%) are depicted in Fig. 2. All CMCS exhibit better  $CO_2$  capture performances than CS, e.g.,  $C_{10}$  of CMCS-5, CMCS-15, and CMCS-25 are 0.62 g/g, 0.43 g/g, and 0.36 g/g, which are 2.18, 1.52 and 1.28 times as high as those of CS, respectively. CMCS-5 exhibits the highest  $C_{10}$  and best cyclic durability during ten cycles. It may be attributed to the support effect on the pore structure of CMCS by adding cement. There is no obvious difference between decrease tendencies in  $CO_2$  capture capacity with cycles of CMCS with different cement addition. On the contrary, the  $CO_2$  capture capacities decrease as the cement addition increases, which may be limited to the reduced CaO that acts as the only active component for  $CO_2$  capture. Thus, CMCS-5 appears more

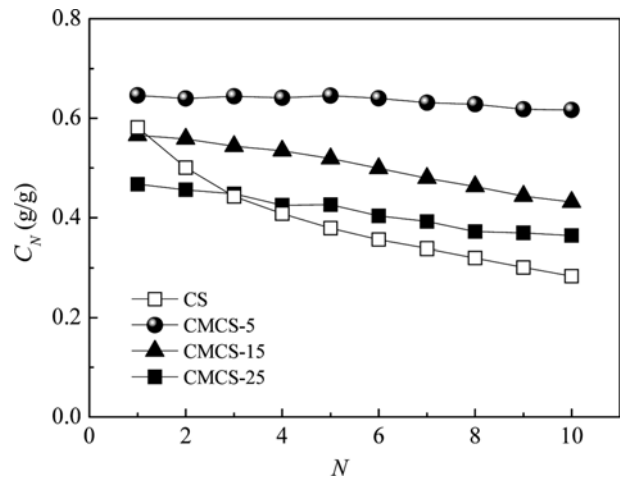


Fig. 2.  $CO_2$  capture capacities of CMCS containing different amounts of cement (preparation: Combustion at 700 °C for 60 min; carbonation: 15%  $CO_2/N_2$ , 700 °C and 20 min; calcination: 99.999%  $N_2$ , 850 °C and 10 min).

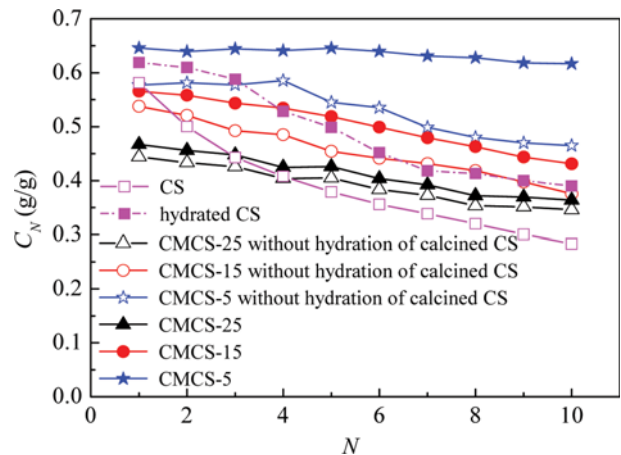


Fig. 3. Effect of hydration of calcined CS in preparation process of CMCS on  $CO_2$  capture capacities (preparation: Combustion at 700 °C for 60 min; carbonation: 15%  $CO_2/N_2$ , 700 °C and 20 min; calcination: 99.999%  $N_2$ , 850 °C and 10 min).

promising and feasible applied in the calcium looping process.

### 2. Effect of Hydration of Calcined CS in Preparation Process of CMCS on $CO_2$ Capture

Effects of hydration step in the preparation on  $CO_2$  capture performance of CMCS are shown in Fig. 3. Obvious increases in the  $CO_2$  capture capacities of both CS and CMCS are observed when the hydration step is applied.  $C_{10}$  of CMCS-5, CMCS-15, CMCS-25 and CS with the hydration step are 33%, 15%, 5% and 38% higher than those without the hydration step, respectively. After the hydration step of calcined CS (the main composition is CaO) in the preparation process of CMCS,  $Ca(OH)_2$  can be generated. During the combustion step,  $Ca(OH)_2$  releases steam and porous CaO is formed. The hydration treatment of CaO is an effective way to improve its porosity and cyclic  $CO_2$  capture capacity in the cycles [31,32] and that is beneficial for  $CO_2$  diffusion and adsorption in CaO. Thus, the hydration step can improve cyclic  $CO_2$  cap-

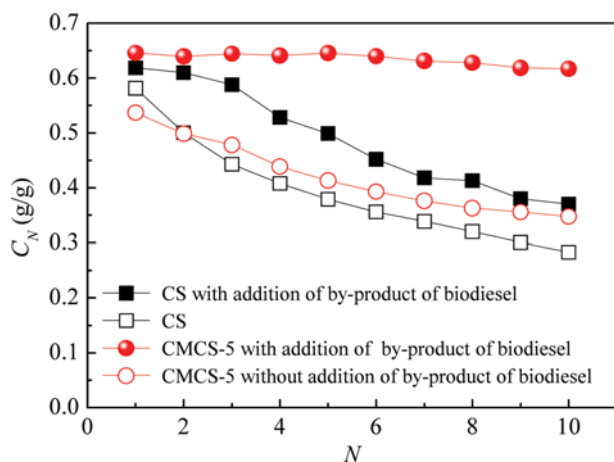


Fig. 4. CO<sub>2</sub> capture capacities of CMCS-5 and CS with and without addition of by-product of biodiesel (preparation: Combustion at 700 °C for 60 min; carbonation: 15% CO<sub>2</sub>/N<sub>2</sub>, 700 °C and 20 min; calcination: 99.999% N<sub>2</sub>, 850 °C and 10 min).

ture capacity of CMCS.

However, as the cement content increases, the influence of hydration step on C<sub>N</sub> of CMCS wears off because of the decrease in CaO content. The hydration step shows the biggest positive impact on the CO<sub>2</sub> capture capacity and cyclic stability of CMCS-5 in the preparation process of CMCS containing various cements. C<sub>10</sub> of CMCS-5 with the hydration step achieves 0.62 g/g. As the cycle number increases from 1 to 10, C<sub>N</sub> of CMCS-5 drops by only 4%, while that of CMCS-5 without the hydration step decreases by 20%. Thus, the hydration step in the preparation process of CMCS leads to a positive effect on the multicyclic CO<sub>2</sub> capture.

### 3. Effect of By-product of Biodiesel Addition in Preparation Process of CMCS on CO<sub>2</sub> Capture

CO<sub>2</sub> capture capacities of CMCS-5 in comparison to CS with and without the addition of by-product of biodiesel in the preparation process are shown in Fig. 4. Compared to CS, C<sub>N</sub> of CS with the addition by-product of biodiesel decreases with the number of cycles in the same tendency but C<sub>10</sub> is 30.6% higher. It is probably attributed to good pore structure formed after rapid combustion process of by-product of biodiesel. Interestingly, C<sub>N</sub> of CMCS-5 is affected more obviously by the addition of by-product of biodiesel. C<sub>10</sub> of CMCS-5 with the addition of by-product of biodiesel is 77.4% higher than that of CMCS-5 without the addition of by-product of biodiesel. The cement addition dramatically improves the cyclic CO<sub>2</sub> capture capacity and durability of the sorbent only after the addition of by-product of biodiesel, e.g., C<sub>N</sub> of CMCS-5 with the addition of by-product of biodiesel decays 5% after ten cycles, while C<sub>N</sub> of CS with the addition of by-product of biodiesel decays 60%. The sintering resistance property is believed to be owing to the inert support material effectively separating CaO particles [33-36]. The by-product of biodiesel is soluble in the water. The Ca(OH)<sub>2</sub> formed after the hydration step can dissolve in the by-product of biodiesel solution. Thus, the good mix of Ca(OH)<sub>2</sub> and cement in the solution is obtained as sol mixing, which leads to evenly mix of CaO and cement in the obtained CMCS. The following study is focused on the CO<sub>2</sub> capture by CMCS with addi-

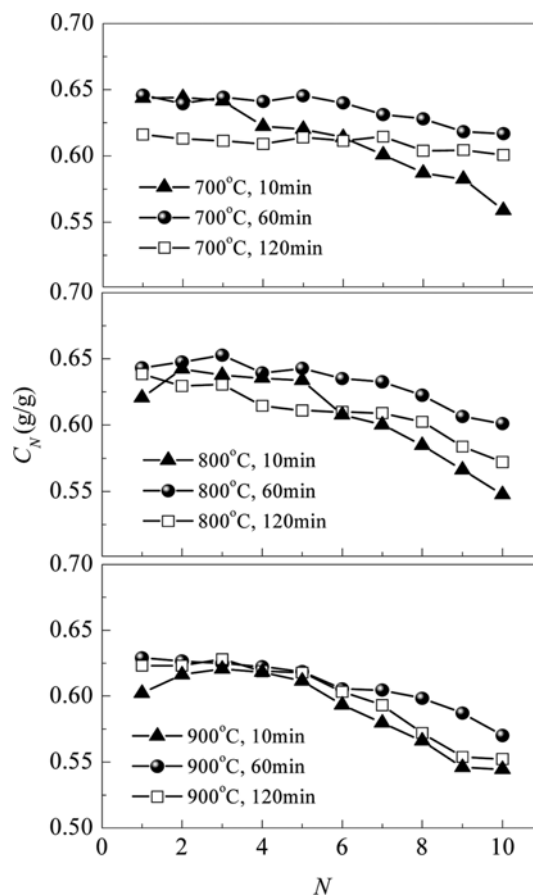


Fig. 5. CO<sub>2</sub> capture capacities of CMCS-5 under different combustion conditions (carbonation: 15% CO<sub>2</sub>/N<sub>2</sub>, 700 °C and 20 min; calcination: 99.999% N<sub>2</sub>, 850 °C and 10 min).

tion of by-product of biodiesel during the preparation process of the synthetic sorbent.

### 4. Effects of Combustion Temperature and Duration in Preparation Process of CMCS on CO<sub>2</sub> Capture

Fig. 5 shows the CO<sub>2</sub> capture capacities of CMCS-5 under different combustion temperatures and durations during the preparation process of the synthetic sorbent. C<sub>N</sub> of CMCS-5 decreases sharply when combustion lasts 10 min. It may be because an unstable structure was formed within a short time, which does not effectively resist sintering. Moreover, the blockage of pores in CMCS-5 occurs to a large extent after 120 min combustion, because longer combustion duration leads to more severe sintering, which is not beneficial for CO<sub>2</sub> capture. CMCS-5 with combustion duration of 60 min forms a stable structure and does not suffer a severe sintering. Therefore, the feasible combustion duration is 60 min in the combustion temperature range of 700-900 °C.

The effect of the combustion temperature during the preparation process on the CO<sub>2</sub> capture behavior of CMCS-5 with combustion duration of 60 min is presented in Fig. 6. C<sub>10</sub> of CMCS-5 decreases as the combustion temperature rises from 700 °C to 900 °C. In the preparation process of CMCS, higher combustion temperature leads to more rapid combustion of the by-product of biodiesel and more complete decomposition of Ca(OH)<sub>2</sub> into CaO. And

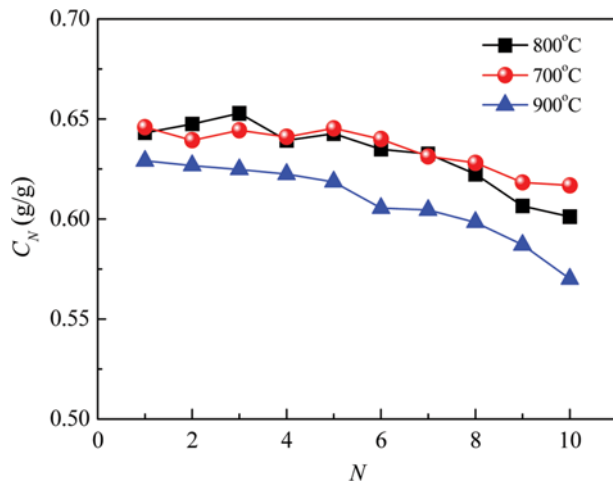


Fig. 6. Effect of combustion temperature on CO<sub>2</sub> capture capacities of CMCS-5 with combustion duration of 60 min (carbonation: 15% CO<sub>2</sub>/N<sub>2</sub>, 700 °C and 20 min; calcination: 99.999% N<sub>2</sub>, 850 °C and 10 min).

then, the porous structure can be obtained due to the gas released from both of the combustion and decomposition processes. However, excessive combustion temperature (e.g., >700 °C) promotes sintering of CMCS, which leads to the blockage and collapse of the obtained sorbent after the combustion. That is not beneficial for CO<sub>2</sub> capture of CMCS. Therefore, the appropriate combustion temperature and the duration during the preparation process of CMCS are 700 °C and 60 min, respectively.

##### 5. Effect of Calcination Temperature on CO<sub>2</sub> Capture Performance of CMCS

Fig. 7 shows the effect of the calcination temperature on CO<sub>2</sub> capture performance of CMCS-5 in ten cycles.  $C_N$  of both CS and CMCS-5 decreases as the calcination temperature increases. As the calcination temperature rises from 850 °C to 950 °C,  $C_{10}$  of CMCS-5 and CS drop by 21% and 22%, respectively. High calcination temperature is the main reason for accelerating the sintering of the sorbents during the calcium looping cycles, which leads to the loss of CO<sub>2</sub> capture capacity eventually [36]. At a high calcination temperature of 950 °C,  $C_{10}$  of CMCS-5 reaches 0.49 g/g, which is 2.21

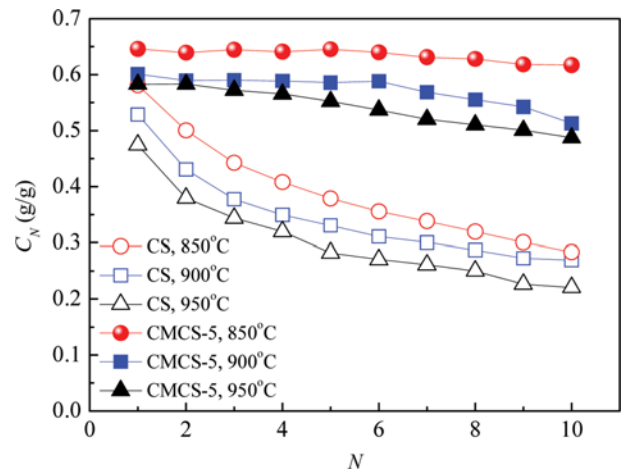


Fig. 7. CO<sub>2</sub> capture capacities of CMCS-5 and CS under different calcination temperatures (carbonation: 15% CO<sub>2</sub>/N<sub>2</sub>, 700 °C and 20 min; calcination: 99.999% N<sub>2</sub> and 10 min).

times as high as that of CS. It indicates that CMCS-5 has better sintering resistance at high calcination temperature.

The CO<sub>2</sub> capture capacities of the synthetic sorbents after ten cycles in the recent literature are summarized in Table 2. The reaction conditions in these researches are fairly similar to those in this study. It is observed that the materials for the preparation of the synthetic sorbents reported are analytical agents such as Al(NO<sub>3</sub>)<sub>3</sub> [14], Ca(NO<sub>3</sub>)<sub>2</sub> and Mn(NO<sub>3</sub>)<sub>2</sub> [37], which are significantly more expensive than CS and cement. The by-product of biodiesel is also a cheaper dispersant compared with C<sub>6</sub>H<sub>8</sub>O<sub>7</sub> reported by Chen et al. [37].  $C_{10}$  of CMCS-5 in our work is 1.28 and 2.2 times as high as those reported in references [38] and [39]. CMCS-5 seems promising as CO<sub>2</sub> sorbent with high activity during the calcium looping cycles.

##### 6. Carbonation and Calcination Behaviors of CMCS in TGA

The carbonation and calcination behaviors of CMCS-5 and CS with the reaction time during the 1st and 11th cycles in TGA are shown in Fig. 8.  $C_N$  of CMCS-5 and CS increase rapidly in the previous 50 s or so and rise slowly over this time, as shown in Fig. 8(a).  $\mu_N$  increases fast with time and reaches the maximum at about 250 s, but it goes down rapidly over this time due to the suppres-

Table 2. Comparison in CO<sub>2</sub> capture capacities of synthetic sorbents reported in references

Sorbent	Ref.	Material/preparation method	CaO content (wt%)	Reaction conditions	$C_{10}$
CMCS-5	This work	CS, cement, by-product of biodiesel/by combustion	95	Carbonation: 700 °C, 15%CO <sub>2</sub> /N <sub>2</sub> , 20 min; calcination: 850 °C, N <sub>2</sub> , 10 min	0.616
CaO/Ca <sub>3</sub> Al <sub>2</sub> O <sub>6</sub>	[14]	CS, Al(NO <sub>3</sub> ) <sub>3</sub> glycerol/by combustion	90	Carbonation: 700 °C, 15%CO <sub>2</sub> /N <sub>2</sub> , 30 min; calcination: 850 °C, N <sub>2</sub> , 10 min	0.455
CaO/MnO <sub>2</sub>	[37]	Ca(NO <sub>3</sub> ) <sub>2</sub> , Mn(NO <sub>3</sub> ) <sub>2</sub> , C <sub>6</sub> H <sub>8</sub> O <sub>7</sub> /by sol-gel method	97	Carbonation: 650 °C, 15%CO <sub>2</sub> /N <sub>2</sub> , 20 min; Calcination: 950 °C, N <sub>2</sub> , 10 min	0.575
CaO/Ca <sub>12</sub> Al <sub>14</sub> O <sub>33</sub>	[38]	Sol-gel CaO, cement/by dry mixing	75	Carbonation: 650 °C, 15%CO <sub>2</sub> /N <sub>2</sub> , 15 min; Calcination: 850 °C, N <sub>2</sub> , 10 min	0.48
CaO/Ca <sub>12</sub> Al <sub>14</sub> O <sub>33</sub>	[39]	Limestone, cement/by wet mixing	90	Carbonation: 650 °C, 15%CO <sub>2</sub> /N <sub>2</sub> , 30 min; Calcination: 900 °C, N <sub>2</sub> , 10 min	0.28

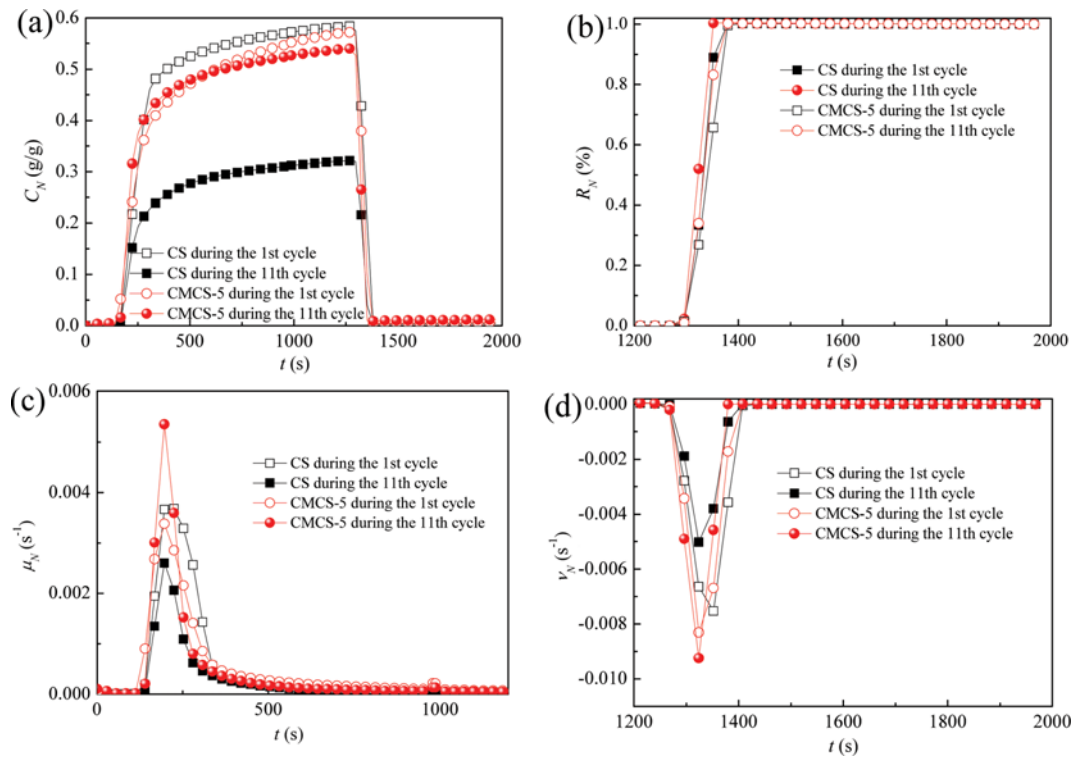


Fig. 8. CO<sub>2</sub> capture behaviors of CMCS-5 and CS with reaction time in TGA: (a) CO<sub>2</sub> capture capacity, (b) decomposition ratio, (c) carbonation rate, (d) calcination rate (carbonation: 15% CO<sub>2</sub>/N<sub>2</sub>, 700 °C and 20 min; calcination: 99.999% N<sub>2</sub>, 850 °C and 10 min).

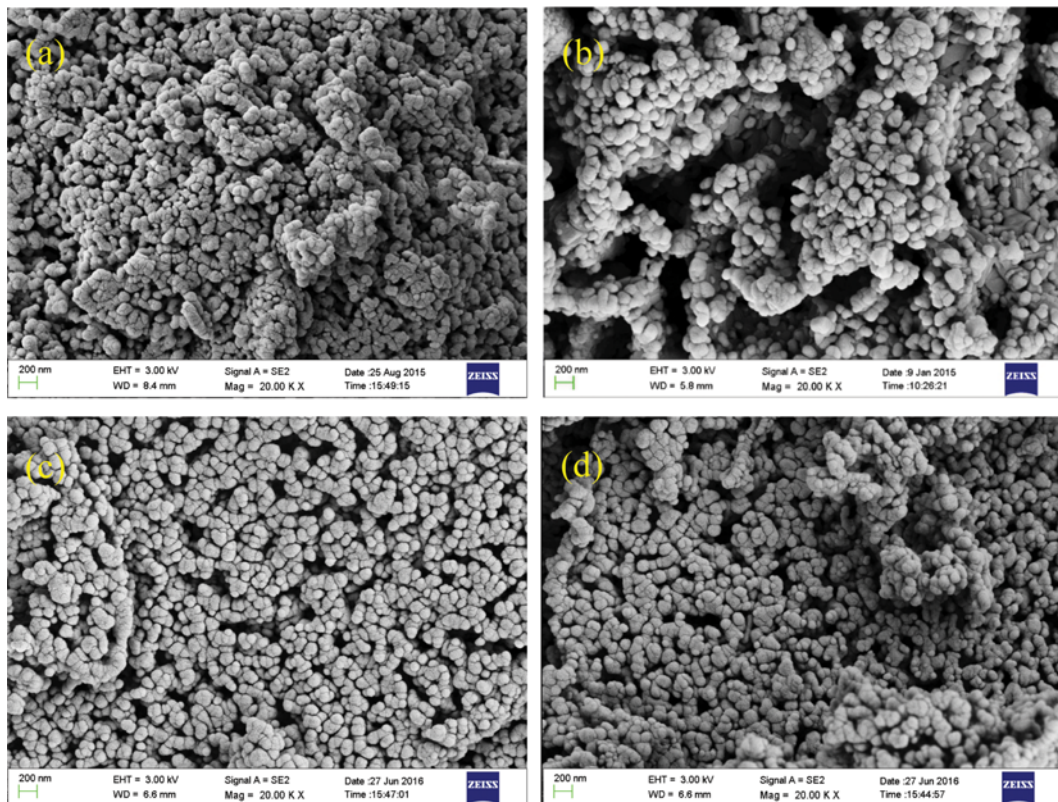


Fig. 9. SEM images of CMCS-5 (combustion at 700 °C for 60 min) and calcined CS (carbonation in 15% CO<sub>2</sub>/N<sub>2</sub> at 700 °C for 20 min, calcination in 99.999% N<sub>2</sub> at 850 °C for 10 min): (a) initial CS after calcination, (b) calcined CS after 10 cycles, (c) initial CMCS-5 and (d) calcined CMCS-5 after 10 cycles.

sion of the thicker carbonation product layer, as plotted in Fig. 8(c). The difference in the carbonation rates of two sorbents is more apparent when the carbonation enters the diffusion controlled stage during the first cycle.  $C_1$  of CMCS-5 gains greater increase during the diffusion controlled stage than that of CS. It may be because of the better pore structure of CMCS-5 which is beneficial for the  $\text{CO}_2$  diffusion and the indepth carbonation. Moreover, CMCS-5 shows higher  $\mu_N$  than CS for the same number of cycles. The maximum  $\mu_{11}$  of CMCS-5 is twice higher, compared to CS, as shown in Fig. 8(c). Both of CS and CMCS-5 decompose completely within 120 s, as shown in Fig. 8(b). Compared with CS in Fig. 8(d), CMCS-5 exhibit higher calcination rate for the same number of cycles, and thus, CMCS-5 needs shorter time for the complete decomposition. Thus, CMCS-5 possesses good  $\text{CO}_2$  absorption and desorption performances.

### 7. Microstructure Analysis

The SEM images of CMCS and CS during ten cycles are compared in Fig. 9. Remarkably, more porous structure in initial CMCS-5 is observed, compared to calcined CS. This is mainly because of numerous pores formed during the combustion of by-product of biodiesel and the dispersion of the cement. Agglomeration and fusion of CaO grains, reduced small pores and increased large pores in CS appear after ten cycles due to the sintering. However, the surface of CMCS-5 after ten cycles makes no difference with that of initial CMCS-5, which indicates that CMCS-5 has higher sintering resistance. It is the more porous and stable pore structure that leads to the better  $\text{CO}_2$  capture performance and cyclic stability of CMCS.

### CONCLUSION

A novel synthetic  $\text{CO}_2$  sorbent prepared from CS as industrial waste, cement and by-product of biodiesel by combustion was proposed. The addition of by-product of biodiesel not only leads to the formation of the porous structure but also makes CaO and cement evenly mixed in CMCS. The optimum additive amount of cement is 5 wt%. CMCS-5 achieves the highest  $\text{CO}_2$  capture capacity, 0.62 g/g after ten cycles, which is 2.2 times higher than that of CS. The optimum combustion temperature and duration in the preparation process of CMCS are 700 °C and 60 min, respectively. CMCS-5 exhibits higher calcination rate for the same number of cycles and, thus, CMCS-5 needs shorter time for the complete decomposition. Thus, CMCS-5 possesses good  $\text{CO}_2$  absorption and desorption performance. It is the more porous and stable pore structure that leads to the better  $\text{CO}_2$  capture performance and cyclic stability of CMCS during the repetitive carbonation/calcination cycles. CMCS appears promising as an effective and low-cost  $\text{CO}_2$  sorbent in the calcium looping.

### ACKNOWLEDGEMENT

Financial support from National Natural Science Foundation of China (51376003), Joint Foundation of National Natural Science Foundation of China and Shanxi Province for coal-based low carbon (U1510130), Primary Research & Development Plan of Shandong Province (2016GSF117001) and the Fundamental Research

Funds of Shandong University, China (2014JC049) is gratefully appreciated. We thank Dr. Hui Li for providing the by-product of biodiesel for this work.

### REFERENCES

1. Z. He, Y. Li and C. Liu, *J. Southeast Univ.*, **31**, 204 (2015).
2. A. Wang, N. Deshpande and L. S. Fan, *Energy Fuel*, **29**, 321 (2015).
3. S. Ackermann, L. Sauvin, R. Castiglioni, J. L. M. Rupp, J. R. Scheffe and A. Steinfeld, *J. Phys. Chem. C*, **119**, 16452 (2015).
4. Q. Wang, N. Rong, H. Fan, Y. Meng, M. Fang, L. Cheng and K. Cen, *Int. J. Hydrogen Energy*, **39**, 5781 (2014).
5. H. R. Radfarnia and A. Sayari, *Chem. Eng. J.*, **262**, 913 (2015).
6. A. L. García-Lario, M. Aznar, I. Martinez, G. S. Grasa and R. Murillo, *Int. J. Hydrogen Energy*, **40**, 219 (2015).
7. X. Zhang, Z. Li, Y. Peng, W. Su, X. Sun and J. Li, *Chem. Eng. J.*, **243**, 297 (2014).
8. M. Broda and C. R. Müller, *Fuel*, **127**, 94 (2014).
9. M. Broda, V. Manovic, E. J. Anthony and C. R. Muller, *Environ. Sci. Technol.*, **48**, 5322 (2014).
10. J. M. Valverde, A. Perejon and L. A. Perez-Maqueda, *Environ. Sci. Technol.*, **46**, 6401 (2012).
11. M. Zhang, Y. Peng, Y. Sun, P. Li and J. Yu, *Fuel*, **111**, 636 (2013).
12. G. Wu, C. Zhang, S. Li, Z. Huang, S. Yan, S. Wang, X. Ma and J. Gong, *Energy Environ. Sci.*, **5**, 8942 (2012).
13. C. Luo, Y. Zheng, N. Ding, Q. Wu and C. Zheng, *Chinese Chem. Lett.*, **22**, 615 (2011).
14. Y. Li, M. Su, X. Xie, S. Wu and C. Liu, *Appl. Energy*, **145**, 60 (2015).
15. M. Kavosh, K. Patchigolla, E. J. Anthony and J. E. Oakey, *Appl. Energy*, **131**, 499 (2014).
16. Z. Zhou, Y. Qi, M. Xie, Z. Cheng and W. Yuan, *Chem. Eng. Sci.*, **74**, 172 (2012).
17. H. Chen, C. Zhao and W. Yu, *Appl. Energy*, **112**, 67 (2013).
18. V. Manovic and E. J. Anthony, *Ind. Eng. Chem. Res.*, **48**, 8906 (2009).
19. V. Manovic and E. J. Anthony, *Environ. Sci. Technol.*, **43**, 7117 (2009).
20. V. Manovic and E. J. Anthony, *Energy Fuel*, **23**, 4797 (2009).
21. C. Qin, J. Yin, H. An, W. Liu and B. Feng, *Energy Fuel*, **26**, 154 (2012).
22. Y. Wu, V. Manovic, I. He and E. J. Anthony, *Fuel*, **96**, 454 (2012).
23. Y. Li, X. Xie, R. Sun and L. Shi, *Proc. Chin. Soc. Electrical Eng.*, **34**, 4447 (2014).
24. Y. Li, W. Wang, X. Cheng, M. Su, X. Ma and X. Xie, *Fuel*, **142**, 21 (2015).
25. R. Sun, Y. Li, J. Zhao, C. Liu and C. Lu, *Int. J. Hydrogen Energy*, **38**, 13655 (2013).
26. Y. Li, R. Sun, C. Liu, H. Liu and C. Lu, *Int. J. Greenh. Gas Con.*, **9**, 117 (2012).
27. X. Ma, Y. Li, L. Shi, Z. He and Z. Wang, *Appl. Energy*, **168**, 85 (2016).
28. W. Liu, H. An, C. Qin, J. Yin, G. Wang, B. Feng and M. Xu, *Energy Fuel*, **26**, 2751 (2012).
29. H. Li, S. Niu, C. Lu, M. Liu and M. Huo, *Sci. China Technol. Sc.*, **57**, 438 (2014).
30. J. C. Thompson and B. B. He, *Appl. Energy*, **22**, 261 (2006).
31. R. W. Hughes, D. Lu, E. J. Anthony and Y. Wu, *Ind. Eng. Chem. Res.*, **43**, 5529 (2004).
32. Y. Li, C. Zhao, C. Qu, L. Duan, Q. Li and C. Liang, *Chem. Eng.*

- Technol.*, **31**, 237 (2008).
33. P. H. Chang, W. C. Huang, T. J. Lee, Y. P. Chang and S. Y. Chen, *ACS Appl. Mater. Int.*, **7**, 6172 (2015)
34. L. Barelli, G. Bidini, A. Di Michele, F. Gallorini, C. Petrillo and F. Sacchetti, *Appl. Energy*, **127**, 81 (2014).
35. C. Luo, Y. Zheng, N. Ding, Q. L. Wu, G. A. Bian and C. G. Zheng, *Ind. Eng. Chem. Res.*, **49**, 11778 (2010).
36. A. Perejón, L. M. Romeo, Y. Lara, P. Lisbona, A. Martínez and J. M. Valverde, *Appl. Energy*, **162**, 787 (2016).
37. H. Chen, P. Zhang, Y. Duan and C. Zhao, *Appl. Energy*, **162**, 390 (2016).
38. C. Luo, Y. Zheng, Y. Xu, H. Ding, C. Zheng, C. Qin and B. Feng, *Korean J. Chem. Eng.*, **32**, 934 (2015).
39. J. Sun, W. Liu, Y. Hu, M. Li, X. Yang, Y. Zhang and M. Xu, *Energy Fuel*, **29**, 6636 (2015).